近紅外光造影技術
fNIRS — Diffuse Optical Imaging

盧家鋒 助理教授
alvin4016@ym.edu.tw

本週課程內容

- Theory of Optical Imaging
- Applications of Optical Imaging

- **In Vivo Optical Imaging of Brain Function.** CRC Press, 2009.
  - Noninvasive Imaging of Cerebral Activation with Diffuse Optical Tomography (chap 14), TJ Huppert, MA Franceschini, DA Boas
- **Application of Near Infrared Spectroscopy in Biomedicine.** Thomas Jue, Kazumi Masuda. Springer, 2013.
  - photo migration (chap 3)

fNIRS光學影像原理
Theory of Optical Imaging

NIRS,DOI, and DOT

- **Near Infrared Spectroscopy (NIRS)**
  - FF Jobsis, 1977, Science
  - Changes in oxy- and deoxy-Hb
- **Diffuse Optical Imaging (DOI)**
- **Diffuse Optical Tomography (DOT)**
  - Spatially resolved imaging
  - Model of light propagation

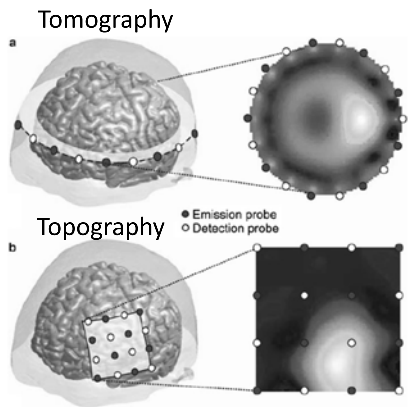

Partial Volume Correction

- Modified Beer-Lambert Law (MBLL)
  - Assumes that changes in chromophore concentrations are spatially uniform over the measurement sampling volume.
- Functional changes
  - Only small portions of the optical sampling volume
  - Correction by a factor of 40 to 60

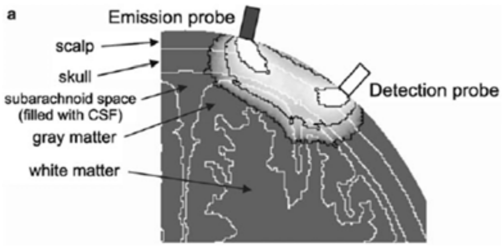

Correction for MBLL

- $\Delta OD(\lambda) = \Delta\mu_a(\lambda)\langle L\rangle = \Delta\mu_a(\lambda)\mathrm{SB}(\lambda)$
  $= [\varepsilon_{HbO}(\lambda)\Delta c_{HbO} + \varepsilon_{HbR}(\lambda)\Delta c_{HbR}]\mathrm{SB}(\lambda)$
  - S : the separation between the source and detector.
  - B(λ) : the pathlength factor, include both a **differential path length factor** (DPF) and a **partial volume factor** for each wavelength.

Diffuse Optical Imaging

- MBLL does not provide a framework for reconstructing images.
- The model of light propagation in tissue is demanded.
- Diffusion approximation

$$-D\nabla^2\phi(r,t) + \mu_a\phi(r,t) + \frac{1}{c}\frac{\partial\phi(r,t)}{\partial t} = S(r,t)$$

DOI and DOT

- A grid arrangement of the optodes determines
  - depth-sensitivity of the measurements
  - Spatial coverage
  - spatial resolution
- For DOT
  - Dense array of optodes
  - Overlapping measurement combinations
  - ➔ **Experimental difficulty (price & time)**

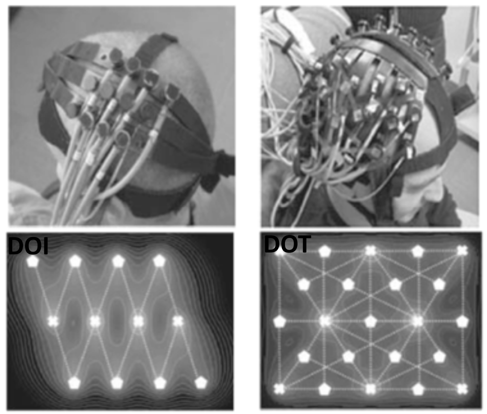

Image reconstruction

- Similar for DOI and DOT
- Forward solver
  - Photon fluence at source and detector positions
- Inverse solver
  - Update $\Delta\mu$

    or Δc_{HbO} and Δc_{HbR}

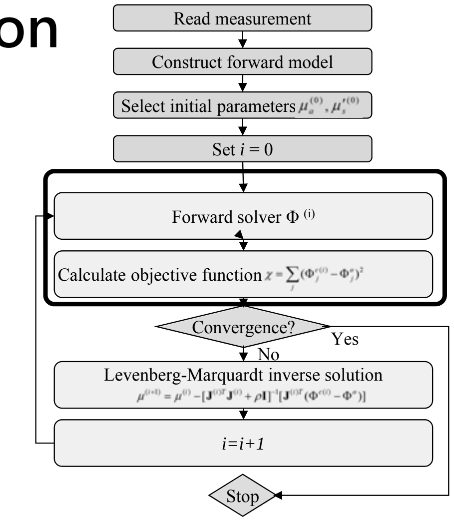

Forward modelling

- Analytic solution
  - Green's solution
- Numerical solution
  - Monte Carlo Simulation
  - Finite Element Method

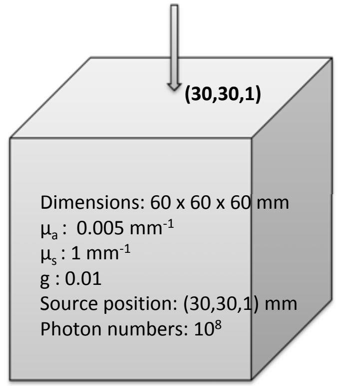

Continuous-wave simulation

- Analytic solution vs. Monte Carlo

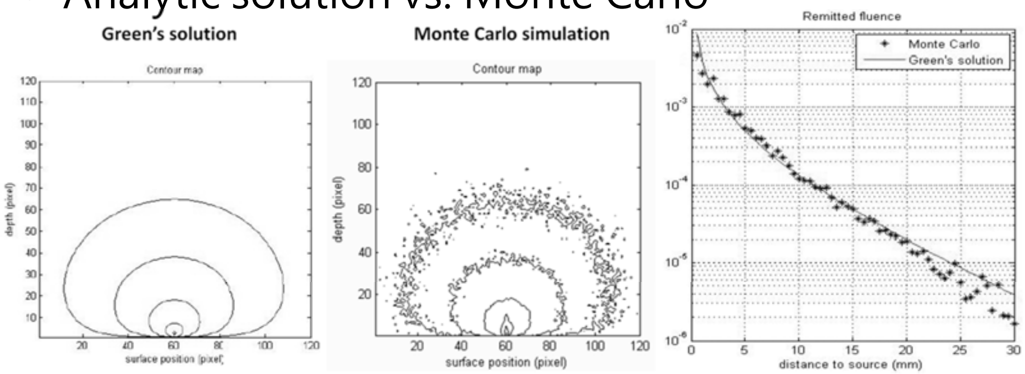

Forward modelling

- Monte Carlo simulation (10^6~10^8 photons) for measuring spatial sensitivity.

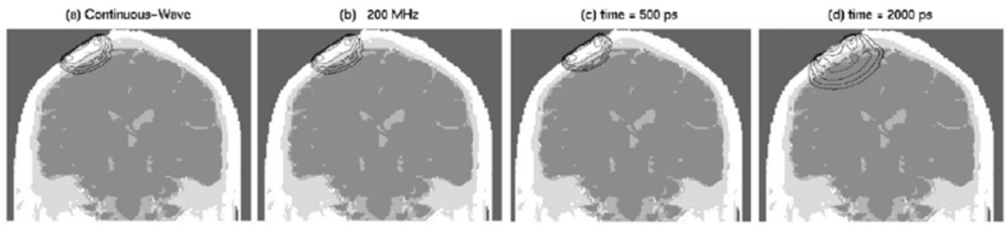

The time-domain sensitivity profiles suggest the possibility of obtaining greater penetration depths in the head from measurements made at longer delay times.

Finite Element Method

- Discretize the area into a set of nodes

$$\Phi = \sum_{i=1}^{N} \Phi_i \Psi_i ,$$

$$K = \sum_{k=1}^{N} \kappa_k \Psi_k ,$$

$$\mu_a = \sum_{l=1}^{N} \mu_l \Psi_l$$

Black: element labeling Red: node labeling

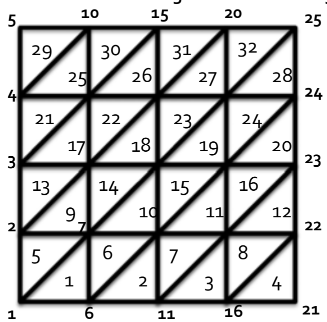

25 nodes, 32 elements

Two dimensional piecewise linear basis

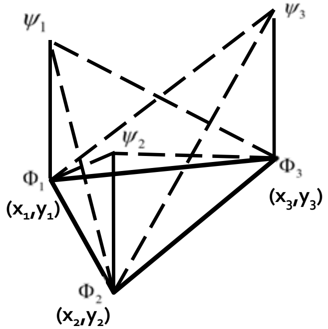

Finite Element Method

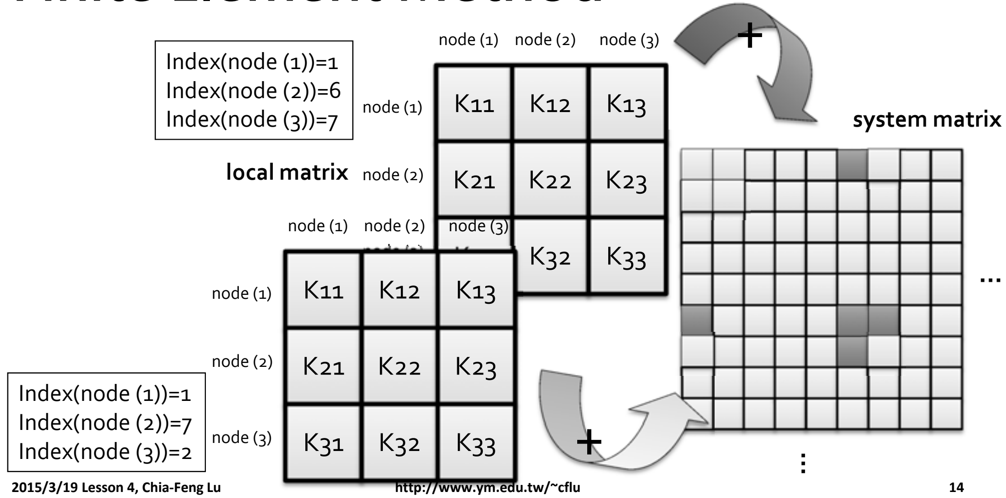

Digital simulation 1/3

- Uniform object μ_s= 1.0mm^{-1}, μ_a=0.002mm^{-1}

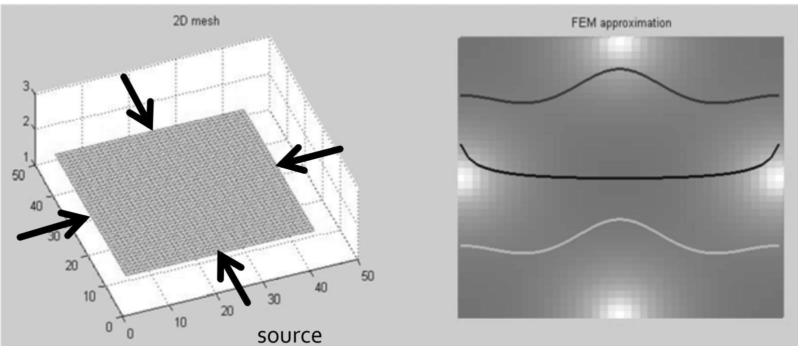

Digital simulation 2/3

- High absorption in center object
  - μ_s= 1.0mm^{-1}, μ_a(1)=0.002, μ_a(2)=0.100 mm^{-1}

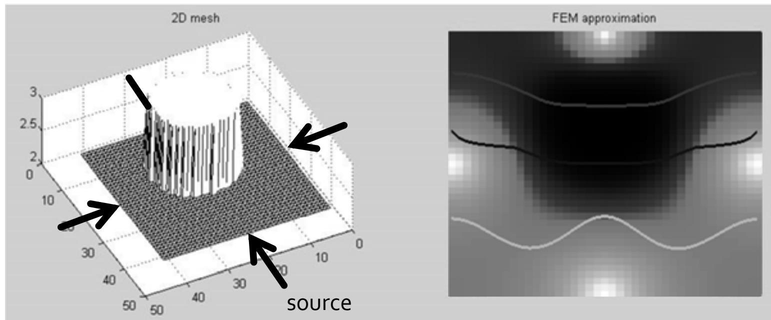

Digital simulation 3/3

- Multi-absorption level object
  - μ_s= 1.0mm^{-1}, μ_a(1)=0.002, μ_a(2)=0.012 , μ_a(3)=0.080 , μ_a(4)=0.050 , μ_a(5)=0.200 mm^{-1}

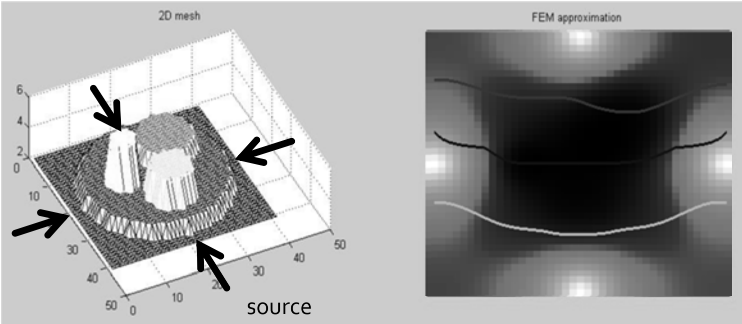

FEM vs MC simulation

- μ_s= 1.0mm^{-1}, μ_a=0.005mm^{-1}, g=0.9, n=1.44

MC simulation | Finite element method

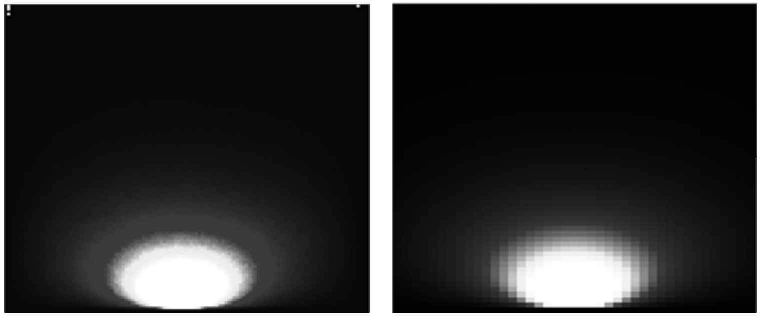

Image reconstruction

- Similar for DOI and DOT
- Forward solver
  - Photon fluence at source and detector positions
- Inverse solver
  - Update $\Delta\mu$

  or Δc_{HbO} *and* Δc_{HbR}

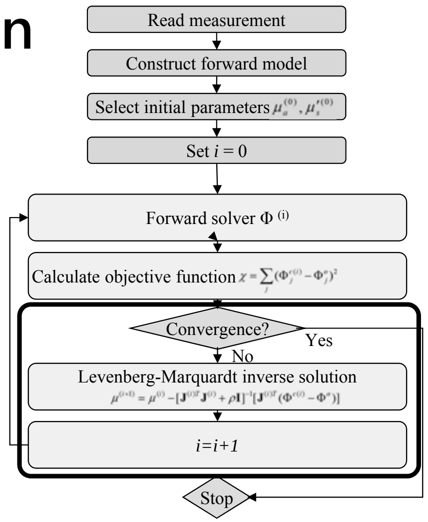

Digital phatom 1/2

μ_s= 1.0mm^{-1}, μ_a(1)=0.002, μ_a(2)=0.100 mm^{-1}

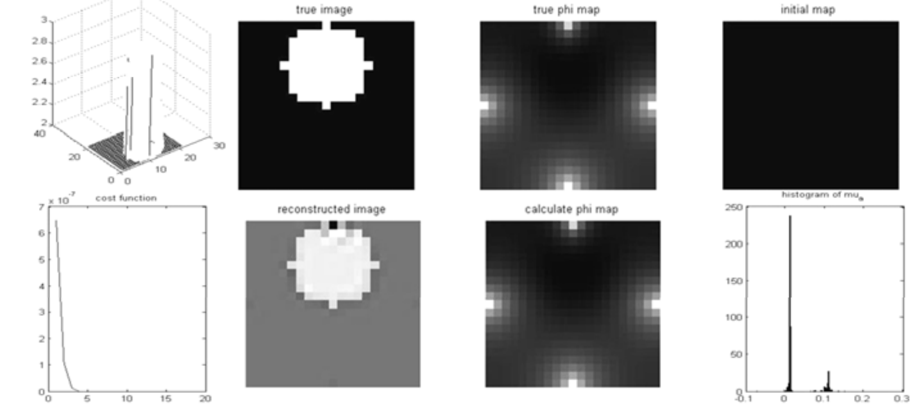

Digital phatom 2/2

- μ_s= 1.0mm^{-1}, μ_a(1)=0.002, μ_a(2)=0.012 , μ_a(3)=0.080 , μ_a(4)=0.050 ,

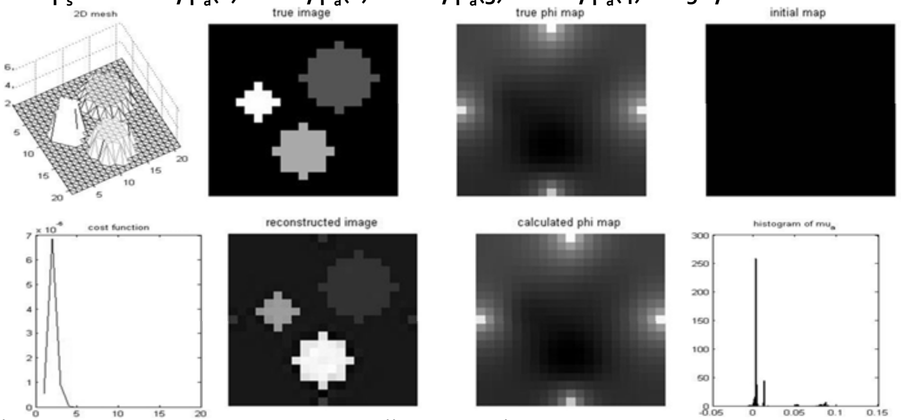

fNIRS影像應用
Applications of DOI/DOT

Instrumentations

- Safety
  - Optical power incident on the tissue <4mW/mm
- Sensitivity
  - Source-detector separation at least 2.5 cm for adults
- Detection
  - 2.5 cm separation → light reaching the detector ~ 10 pW
  - Need PMT, avalanche photodiodes (APD) or CCD cameras

Imaging Instrumentation

- More sources and detectors compared to NIRS
  - Each detector operates independently.
  - The source light must be encoded.
- Encoding strategies
  - **Time-sharing**: turn on one source at a time (10-100 ms)
  - **Time-encoding**: faster switching rate (<100μs) and integrating over several switch cycles
  - **Frequency-encoding**: modulate sources at different frequency and recognized by a digital band-pass filter

Comparison of image reconstruction

- Only the tomography image reveals the two absorbers with equal amplitude.

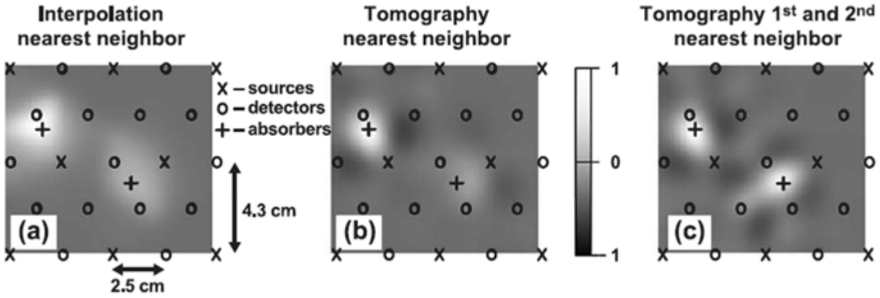

Digital Simulation

- (b) True location of the simulated absorption change. (c) Image reconstructed using DOT and overlapping measurements. (d) Image reconstructed with a cortical constraint

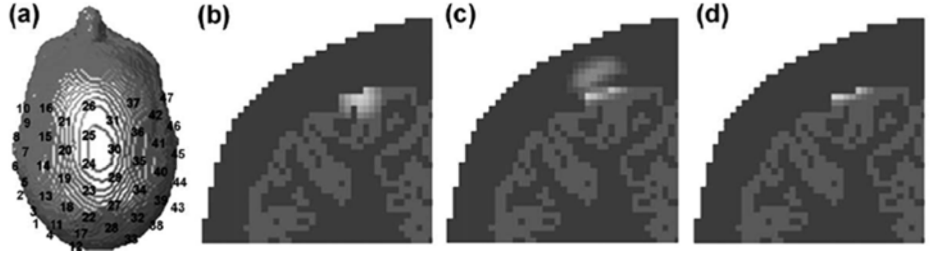

DOI recording on M1

< finger taping > Rescaled and normalized signals

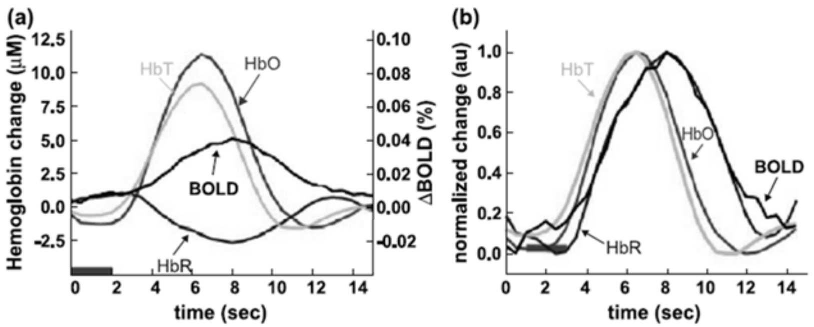

DOI and fMRI activations

fMRI activations

Corresponding Hb dynamics

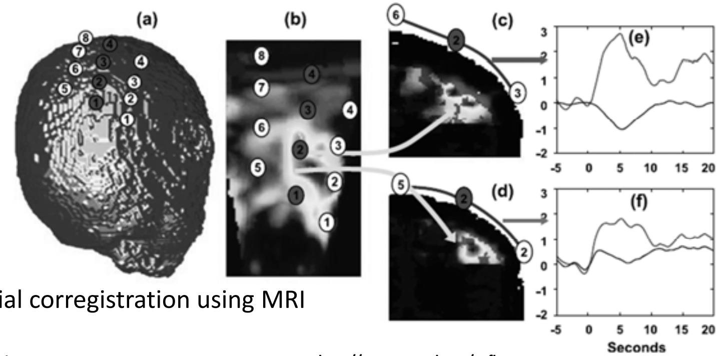

HbO
HbR

Spatial coregistration using MRI

DOT with visual stimulus

- Contrast-reversing checker board pattern

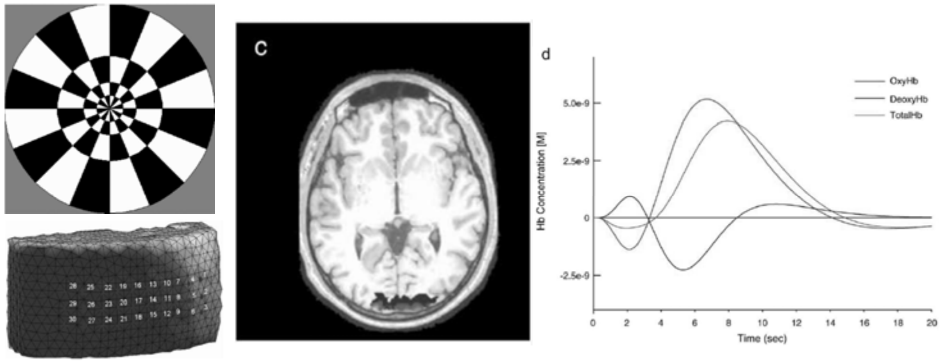

DOT Applications

Neomatal brain

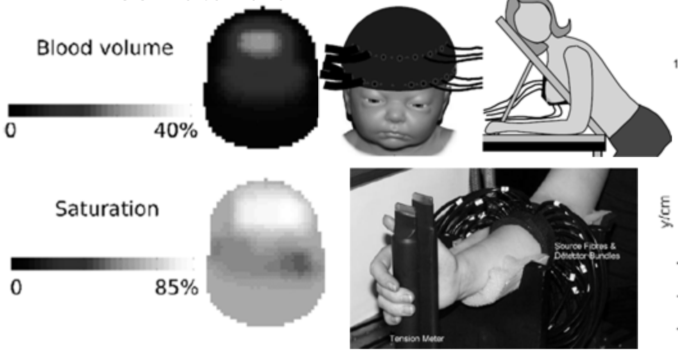

Optical mammography

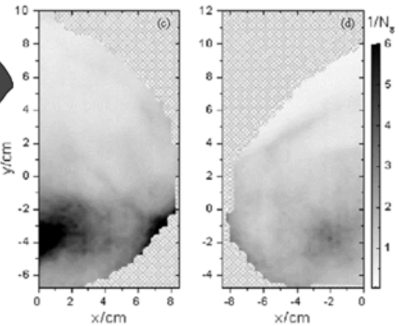

THE END

alvin4016@ym.edu.tw